



Category: STEM (Science, Technology, Engineering and Mathematics)

ORIGINAL

## Forced convective rate and pressure drop through a packed annulus: a numerical simulation

### Velocidad de convección forzada y caída de presión a través de un anillo relleno: simulación numérica

Noor Sabah Falieh<sup>1</sup> , Saad Najeeb Shehab<sup>1</sup> 

<sup>1</sup>Mechanical Engineering Department, College of Engineering, Mustansiriyah University. Baghdad, Iraq.

Cite as: Sabah Falieh N, Najeeb Shehab S. Forced convective rate and pressure drop through a packed annulus: a numerical simulation. Salud, Ciencia y Tecnología - Serie de Conferencias. 2024; 3:845. <https://doi.org/10.56294/sctconf2024845>

Submitted: 28-01-2024

Revised: 14-04-2024

Accepted: 04-06-2024

Published: 05-06-2024

Editor: Dr. William Castillo-González 

Note: Paper presented at the 3rd Annual International Conference on Information & Sciences (AICIS'23).

#### ABSTRACT

Porous materials are used in engineering and industry due to their heat transmission qualities. This study examined forced convection flow through an annular tube packed with sphere balls of various materials and sizes using numerical analysis. The sphere balls were permeable. Ceramic, plastic, and steel with spherical diameters of 3, 5, and 6 and porosity of 0,4 were tested for heat dissipated and fluid flow. Also, test the impact of steel balls of diameter 6mm with 0,6 and 0,8 porosity. The numerical simulation results are used to analyze the forced convection and fluid flow parameters of a three-dimensional annular tube with continuous heat flux in the Reynold number range (5 000-14 000). Steel balls had an 80 % higher heat transfer coefficient than annular tubes without porous mediums. The simulation showed that inserting the porous media increased annular tube pressure loss. The maximum heat transfer coefficient improved by about 80 % when the spherical diameter is 3 mm. Also, the result illustrated the heat transfer coefficient of steel balls Increased by about 79 %, 69 %, and 49 %, with 0,4, 0,6, and 0,8 respectively.

**Keywords:** Packed Annulus; Forced Convective; Porous Medium; Simulation; Pressure Drop.

#### RESUMEN

Los materiales porosos se utilizan en ingeniería e industria debido a sus cualidades de transmisión de calor. En este estudio se examinó el flujo por convección forzada a través de un tubo anular relleno de bolas esféricas de distintos materiales y tamaños mediante análisis numérico. Las esferas eran permeables. Se ensayaron bolas de cerámica, plástico y acero con diámetros esféricos de 3, 5 y 6 y porosidad de 0,4 para determinar el calor disipado y el flujo de fluido. También se probó el impacto de bolas de acero de 6 mm de diámetro con porosidad de 0,6 y 0,8. Los resultados de la simulación numérica se utilizan para analizar los parámetros de convección forzada y flujo de fluidos de un tubo anular tridimensional con flujo de calor continuo en el intervalo de números de Reynold (5 000-14 000). Las bolas de acero presentaron un coeficiente de transferencia de calor un 80 % superior al de los tubos anulares sin medio poroso. La simulación demostró que la inserción del medio poroso aumentaba la pérdida de presión del tubo anular. El coeficiente máximo de transferencia de calor mejoraba en torno a un 80 % cuando el diámetro esférico era de 3 mm. Asimismo, el resultado ilustró que el coeficiente de transferencia de calor de las bolas de acero aumentó en torno al 79 %, 69 % y 49 %, con 0,4, 0,6 y 0,8 respectivamente.

**Palabras clave:** Anillo de Empaquetamiento; Convección Forzada; Medio Poroso; Simulación; Caída de Presión.

## INTRODUCTION

Convection heat transfer and fluid flow in the backed annulus are significant phenomena in engineering systems. These phenomena find their technological applications in various fields, including heat exchangers, nuclear reactors, thermal storage systems, aircraft fuselage insulation, underground electrical transmission cables, solar energy systems, boilers, cooling of electronic devices, compact heat exchangers, and cooling cores of nuclear reactors.<sup>(1,2,3)</sup>

Numerous researchers have investigated the forced convection flow through porous media using a variety of numerical and experimental techniques.

Prak H. Jadhav et al.<sup>(4)</sup> evaluated heat exchanger pressure drop and heat transmission with partially filled high-porosity aluminum and copper foams. M1, M2, and M3 are partially filled with positive (increasing, 20/45 PPI), negative (decreasing, 45/20 PPI), and compound (45 Cu/20 Al PPI) graded porous layer thickness. Their inner diameters are 0,06 m, 0,04 m, and 0,02 m, respectively, and their outer diameters are 0,10 m. M1 and M2 with decreasing graded metal foam had 1,68 %-12,85 % and 13,42 %-23,32 % higher heat transfer rates than M2 and M3 without it due to 55,43 %-84,02 % and 35,69 %-50,31 % reduced pumping power.

Shicheng wang et al.<sup>(5)</sup> used many numerical simulations to describe particle-scale heat transmission in packed mattresses. They developed direct heat transmission technology for such beds. CFD handles the gas problem continuously, while DEM solves the particle problem discretely. Heat transfer is assessed using entrance dissipation. Data shows that radial multiparticle size distribution promotes heat transmission more than uniform particle size distribution. It optimises velocity and temperature, reduces convective heat transfer equivalent thermal resistance, and dramatically raises outlet gas temperature. Increased distribution thickness boosts heat transmission without lowering bed thermal resistance.

K.S.Bibin et al.<sup>(6)</sup> calculated forced convective heat transfer and pressure drop in a square duct's entry and fully formed sections partially filled with porous medium. Porous media is near the wall or square duct core. Heat transfer and pressure drop are improved by adding wire mesh screens at the duct core. Maximum wall-side heat transmission is 1,65 times that of a non-porous duct at thickness ratios of 0,8-1,0. Wall-side porosity increases Nusselt number. Reduced porosity raises Nusselt number in core-side porous medium.

Jian Yang et al.<sup>(7)</sup> studied flow and heat transmission inside microscopic holes of structured packed beds of dimple particles using numerical study. The packed bed with dimple particles has a higher heat transfer efficiency and lower pressure drop and heat transmission than the one with smooth particles. True even with the same inlet velocity.

Shiyang Li et al.<sup>(8)</sup> Numerical analysis Smooth or dimpled spheres in structured packed beds for fluid flow and heat transfer. Identification of complex dimpled structural effects on heat transmission and flow. Selected low channel-to-particle diameter ratios were 1,00 and 1,15. Falling pressure revealed Nusselt amount. Dimpled spheres in the structured packed bed result in a slightly higher Nusselt number at  $1\ 500 < ReH < 14\ 000$  and smaller pressure drop at  $N = 1,00$  compared to smooth spheres. Heat is transferred by the dimpled sphere-packed bed. Structured packed beds with dimpled spheres have a larger pressure drop at  $N = 1,15$ , lowering heat transfer efficiency. Topologies lower drag differentially and heat transfer rises little when comparing channel-to-particle diameter ratios.

Sauce Aksornkitti et al.<sup>(9)</sup> employed two-dimensional unsaturated flow and heat transfer models to numerically analyse hot water infiltration transport in a two-dimensional granular packed bed.

Isbeyeh W.maid et al.<sup>(10)</sup> utilised ANSYS FLUENT 14,1 to model twin tube heat exchanger heat transfer with and without porous media. 2,5 mm porous alumina Double-tube heat exchanges using water. As the mass flow rate ratio increases, adding a porous pad increases heat exchanger efficiency and heat transmission, with the highest value when alumina is in double pipe. Mass flow rate ratio decreases effectiveness, while alumina as a porous media improves IOP, IP, OP, and NP, increasing NTU efficacy.

Irfan Anjum Badruddin et al.<sup>(11)</sup>, examined the concentrated heat transfer properties in a porous duct made up of a square duct with its inner walls exposed to a cool temperature ( $T_c$ ) and its outer walls exposed to a hot temperature ( $T_h$ ). They focus on examining the Nusselt number for specific duct ratio values that oscillate over the porous medium's width at the cavity's bottom wall.

W.zhang et al.<sup>(12)</sup> Examined how well different porous mediums transfer heat when subjected to equal pumping power. used pore sizes and aluminium metal foams with varying porosity ranges to channel half-height ratio It has been discovered that, in the region of moderate pumping power, the traditional local thermal equilibrium model significantly overestimates the Nusselt number, particularly when large-pore metal foam is utilised to fill the channel.

Mehmet et al.<sup>(13)</sup> studied porous medium consists of 3 mm steel balls enclosed in a 51,4 mm inner diameter pipe. Heat is applied to the exterior surface of the pipe at a rate of approximately 7,5 kW/m<sup>2</sup> using electrical ribbon heaters. If all the parameters are set appropriately, Comsol provided reliable results in heat transfer problems over porous media, saving money and time on building costly experimental rigs and conducting experiments.

Huijin Xu et al.<sup>(14)</sup> analysed fully developed forced convective heat transfer in an annulus filled with porous media heated asymmetrically using several models. The five models' inner and outer wall important heat flux (HF) ratios were depicted as Nu-curves. These solutions anticipate thermal performance for an asymmetrically heated circular tube filled with a porous material at various radii and HF ratios.

Hikmat N et al.<sup>(15)</sup> Three-diameter forced convective heat transfer in a vertical channel utilising spherical glass. When Reynolds number increased by 65 % and heat flux by 71 %, local Nusselt number increased by 34 % and 11 %. Increased particle diameter increases heat transfer rate from 1 to 3 mm but decreases from 3 to 10 mm. Porosity rises 23 % and channel pressure drop falls 97 %.

Ahmed A. Mohammad et al.<sup>(16)</sup> conducted experiments Heat transfer via forced convection in ducts with porous media (cross-sections that are circular, triangular, or rectangular) The experimental findings showed empirical correlations for the average Nusselt number and Peclet number, as well as the effects of Reynolds number and cross-section on the temperature profile and local Nusselt number for three ducts.

Thaer H. Farhan et al.<sup>(17)</sup> improved heat exchanger performance by filling the gap between the pipes with metal foam (MF). The test segment had two concentric pipes. The MF heat exchanger outperformed the smooth heat exchanger in thermal performance in all configurations, and the greater Nusselt number (Nu) was at or near 50 °C.

O.H. Hassan et al.<sup>(18)</sup> tested forced convection of turbulent flow in a 500-length, 47-width cylinder channel packed with steel spheres and heated by electromagnetic induction. This is air-based. Sphere diameter  $d=6,8,10$ , and 14 mm, red spans 490-5 490 mm. Increasing (Red) enhances heat transfer at the same porosity, and lowering the channel by 6 % increases heat transmission by 38 %. A 6 % porosity decrease doubles pressure drop at Red. At the same porosity, 100 % Red doubles pressure decrease.

Suhad A. Rasheed et al.<sup>(19)</sup> presented an experimental study of the effect of change heater section (circular , square, triangular) on the forced convection heat transfer through a duct packed with glass balls under laminar steady flow, the results showed best improvement in heat transfer for circular cylinder (63 %), square cylinder (71 %), and triangular cylinder(74 %).

Yousif et al.<sup>(20)</sup> employed vertical annuli tubes with three glass balls of different diameters and porosities. The experimental results show that ball size and porosity reduce increase Nusselt number. For constant porosity, annuli with vertical porous media have forced heat convection performance three to three and a half times higher Nusselt number than annuli without porous media.

This study will demonstrate how the performance of heat transfer is affected by turbulent forced convection in concentric annuli containing sphere balls of different materials, sizes, and porosities.

## Numerical simulation

### Physical model

The first step in any investigation is to design a model. After conducting extensive research, we have decided on a concentric annular tube model that is filled with sphere particles (steel, ceramic, PVC balls) as porous media, as seen in figure 1. This study aims to demonstrate how the efficiency of heat transfer is affected by the rate of water entering the packed annular tube, as opposed to the traditional method. That uses various porous materials and diameters for each test. In this model, cold water flows through the outer tube's annular pipe, while a heat source is placed in the inner pipe.

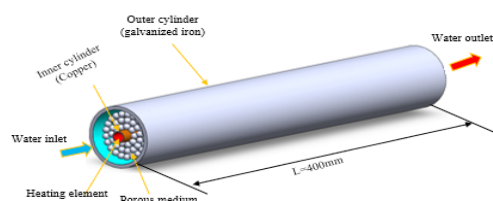


Figure 1. The test section of the present model

As shown in figure 1, test section comprises inner and outer tubes with a length of 400 mm. The outer tube is made of galvanized iron and has outer and inner diameters of 61 mm and 54 mm, respectively. The inner tube

is made of copper, with an outer diameter of 12 mm and an inner diameter of 10 mm. The electrical cylinder heater inserted inside the inner tube has a diameter of 10 mm and a length of 400 mm. The sphere particulars fill the gap between the two pipes. The working fluid is water, which enters the test section at a temperature of 300 K.

The model was designed and analyzed using the commercial software ANSYS-FLUENT. The 3-D Navier-Stokes equation was utilized to discretize the fluid domain. The flow was assumed to be steady, incompressible, and three-dimensional. Since the Reynolds number range (5 000-14 000), The k- $\omega$  (SST) turbulence model was utilized to simulate turbulent flow in this investigation. The radiation heat transfer is neglected since the outer tube is assumed to be insulated.

### Mesh generation and mesh independence

For this analysis, a mesh was created using ANSYS FLUENT R19 and the multizone mesh method for both the solid and fluid domains. The mesh for the current model is shown in.<sup>(21)</sup> The accuracy of the numerical results depends on the size of the elements, so they were gradually reduced to make the mesh finer until the results stopped changing. To save time, the numerical results were obtained using a lower grid number. The element numbers 1 941 420 and node 1 956 816 in.<sup>(22)</sup> Show that the results remain constant in the model being studied

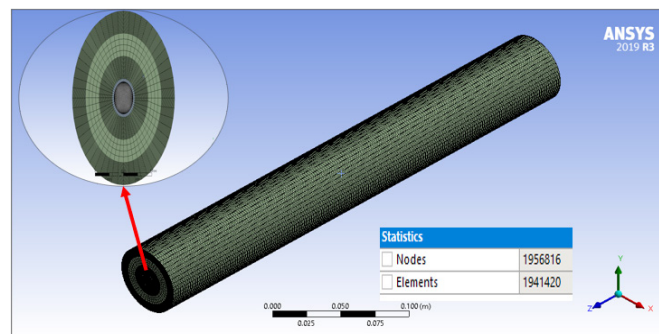


Figure 2. The mesh of the geometry

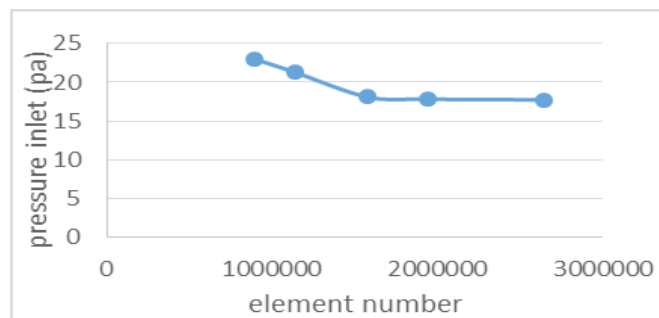


Figure 3. Grid independency

### Governing equation

It is important to state the governing equations and clarify the assumptions regarding the type of flow and working fluid to simplify the numerical process.

The following assumptions are adopted:

- ✓ Steady state
- ✓ Incompressible fluid
- ✓ Turbulent flow with Reynold range (5 000-14 000)
- ✓ Force convection heat transfer
- ✓ Negligible radiation heat transfer losses

So the following equations of energy, momentum mass conservation will be used: <sup>(15,23,24,25)</sup>

➤ Continuity equation

$$\frac{\partial \bar{u}}{\partial x} + \frac{\partial \bar{v}}{\partial y} + \frac{\partial \bar{w}}{\partial z} = 0 \quad (1)$$

➤ The momentum equation

The momentum equation in the x-direction:

$$\frac{1}{\varepsilon^3} \left[ u \frac{\partial u}{\partial x} + v \frac{\partial v}{\partial y} + w \frac{\partial w}{\partial z} \right] - \frac{1}{\rho_f} \frac{\partial p}{\partial x} + \frac{1}{\varepsilon^2} v_{eff} \left( \frac{\partial^2 u}{\partial x^2} + \frac{\partial^2 u}{\partial y^2} + \frac{\partial^2 u}{\partial z^2} \right) - \frac{v_f}{K_f} + \frac{\varepsilon c}{\sqrt{k_f}} |\vec{V}| \quad (2)$$

The momentum equation in y-direction:

$$\frac{1}{\varepsilon^3} \left[ u \frac{\partial u}{\partial x} + v \frac{\partial v}{\partial y} + w \frac{\partial w}{\partial z} \right] = - \frac{1}{\rho_f} \frac{\partial p}{\partial y} + \frac{1}{\varepsilon^2} v_{eff} \left( \frac{\partial^2 v}{\partial x^2} + \frac{\partial^2 v}{\partial y^2} + \frac{\partial^2 v}{\partial z^2} \right) - \left[ \frac{v_f}{K_f} + \frac{\varepsilon c}{\sqrt{k_f}} |\vec{V}| \right] v \quad (3)$$

The momentum equation in z-direction:

$$\frac{1}{\varepsilon^3} \left[ u \frac{\partial u}{\partial x} + v \frac{\partial v}{\partial y} + w \frac{\partial w}{\partial z} \right] = - \frac{1}{\rho_f} \frac{\partial p}{\partial z} + \frac{1}{\varepsilon^2} v_{eff} \left( \frac{\partial^2 w}{\partial x^2} + \frac{\partial^2 w}{\partial y^2} + \frac{\partial^2 w}{\partial z^2} \right) - \left[ \frac{v_f}{K_f} + \frac{\varepsilon c}{\sqrt{k_f}} |\vec{V}| \right] w \quad (4)$$

➤ Energy equation

$$\mathbf{u} \frac{\partial T}{\partial x} + \mathbf{v} \frac{\partial T}{\partial y} + \mathbf{w} \frac{\partial T}{\partial z} = \frac{k_{eff}}{(\rho C_p)_f} \left( \frac{\partial^2 T}{\partial x^2} \right) + \left( \frac{\partial^2 T}{\partial y^2} \right) + \left( \frac{\partial^2 T}{\partial z^2} \right) \quad (5)$$

### Boundary conditions

The boundary conditions were applied to the test section, selecting velocity inlet, pressure outlet (open to atmosphere), and insulated outer pipe. The fluid domain was porous (0,4, 0,6, 0,8). In porous zones, permeability and inertial resistance must be calculated:<sup>(24)</sup>

$$k = \frac{\varepsilon^3 d^2}{175} (1 - \varepsilon)^2 \quad (6)$$

Where  $k$  is the permeability [ $m^2$ ],  $\varepsilon$  is the porosity, and  $d$  is the particle diameter. And the inertial resistance calculate from the following formula.

$$i = \frac{3.5(1-\varepsilon)}{d \cdot \varepsilon^3} \quad (7)$$

The heat flux was applied to the inner surface of the inner pipe with 33 113  $w/m^2$ . The table 1 illustrate the boundary conditions.

Table 1. The boundary conditions	
Domain	Boundary condition
Inlet	Velocity inlet [ $m \cdot s^{-1}$ ]
Outlet	Pressure outlet [pa]
Water	Porous zone
Inner pipe	Heat flux

Since the flow is turbulent the  $k-\omega$  (SST) turbulence model was used in all the simulations in this study.<sup>(25)</sup> Furthermore, the pressure-velocity coupling was solved using the SIMPLE approach. The pressure, velocity, and energy were discretized as second-order upwind.<sup>(26)</sup>

### Mathematical model

The equation below can be used to compute the Reynolds number value, which is how we can determine the type of flow in the annuli.<sup>(15,27)</sup>

$$Re = \frac{\rho_w u_w D_h}{\mu_w} \quad (8)$$

Where  $u_w$  is the average inlet water velocity (m/s),  $\rho_w$  is the water density ( $kg/m^3$ ),  $\mu_w$  is the viscosity of the water. And  $D_h$  is the hydraulic diameter and it defined as:

$$D_h = \frac{4A_c}{P_w} \quad (9)$$

Where:  $A_c$  and  $P_w$  are the cross sectional area and wetted perimeter of the annuli. The average heat transfer coefficient is defined as:

$$\bar{h} = \frac{q''}{T_{s,av} - T_b} \quad (10)$$

Where ( $q''$ ) is the heat flux  $W/m^2$ , ( $T_b$ ) is the water bulk temperature (K), and  $T_{s,av}$  is the average surface temperature (K). The average Nusselt number is obtained as:<sup>(16)</sup>

$$\overline{Nu} = \frac{\bar{h} D_h}{k_{eff}} \quad (11)$$

Where  $K_{eff}$  is the effective thermal conductivity and it's given as:

$$k_{eff} = \epsilon \cdot k_w + (1 - \epsilon) k_p \quad (12)$$

Where  $k_w$  and  $k_p$  are the thermal conductivity of water and porous media (steel) respectively,  $\epsilon$  is the porosity of the porous medium.

$$\epsilon = \frac{V_d - V_p}{V_d} \quad (13)$$

Since  $V_p$  is the porous media sphere volume ( $m^3$ ) and  $V_d$  is the annual volume and it gives as:

$$V_d = \left(\frac{\pi}{4} D_h^2 L\right) \quad (14)$$

Where  $L[m]$  is the length of the test section.

The friction factor can be calculated as:

$$f = \frac{\Delta p}{L} \cdot \frac{d_p}{\rho u^2} \cdot \frac{\epsilon^3}{1 - \epsilon} \quad (15)$$

Since  $\Delta p$  is the pressure drop across the porous medium channel (pa), and  $d_{pthe}$  porous particles diameter (m).

**The properties of porous media are study**

The pvc, ceramic and steel balls are the porous medium is used in this study and its diameters, thermal conductivity, permeability and porosity are illustrated in table 2 the effective thermal conductivity is calculated from equation 6.

Table 2. the properties of porous media are study				
Material	Effective thermal conductivity ( $K_{eff}$ ) (W/m <sup>2</sup> . K)	Diameter (m)	Permeability K(m <sup>2</sup> )	Porosity
Pvc	0,336	3	2,962×10 <sup>-9</sup>	0,4
		5	8,22×10 <sup>-9</sup>	
		6	1,18×10 <sup>-8</sup>	
Ceramic	0,378			
Steel	9,84	3	2,962×10 <sup>-9</sup>	0,4
		5	8,22×10 <sup>-9</sup>	
		6	1,18×10 <sup>-8</sup>	0,4
			1,18×10 <sup>-8</sup>	0,6
			5,26×10 <sup>-9</sup>	0,8

**RESULTS AND DISCUSSIONS**

This analysis examines how porous media affects inner circular cylinder convective heat transfer. Ceramic, plastic, and steel balls with sizes of 3, 5, and 6 mm. The temperature contour, velocity vector, and pressure drop were obtained at Reynold numbers (5 000, 6 000, 8 000, 10 000, 12 000, and 14 000) using commercial software ANSYS fluent version 2019 R3, with water velocities of (0,102, 0,122, 0,16, 0,203, 0,24, and 0,285) m/s and constant heat flux of 33113 W/m<sup>2</sup>.

**Validation**

The Nu number through the test portion was compared with another researcher's.<sup>(24)</sup> As shown in figure 4 The present study shows good agreement with; the value of the Nu number grows with the increase of the Re number. Furthermore, the current numerical results and previous study matched well with the experimental data in the previous study at a porosity of 0,75 and sphere diameter of 16 mm as appear in figure 4.

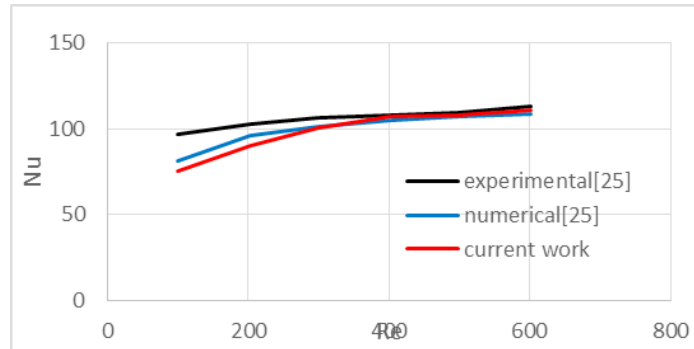


Figure 4. Nu validation

**Temperature distribution**

The study considered the temperature distribution within an annular tube filled with a porous medium that exists between the outer and inner tube surfaces of the solid and liquid sections at inlet temperature 300 k and constant heat flux 33 113 [w/m<sup>2</sup>] and the value of Reynold number 5000. Figure 5 demonstrates that the inserted porous medium increases the temperature distribution and how changes in the material type of the porous medium (ceramic, plastic, steel) impact the temperature distribution while maintaining a constant porosity and diameter. The plane was taken to the (y,z) along the annular tube. The thermal flow that appears in the layer contacts the inner tube and begins to increase gradually towards the z-axis. The water gains the heat from the inner tube and this heat transferred from the inner tube to the water increases when insert porous medium and the amount of heat transferred is affected by the material of the porous medium. Steel material has the highest heat transfer than plastic and ceramic because it has high thermal conductivity as seen in figure 5.

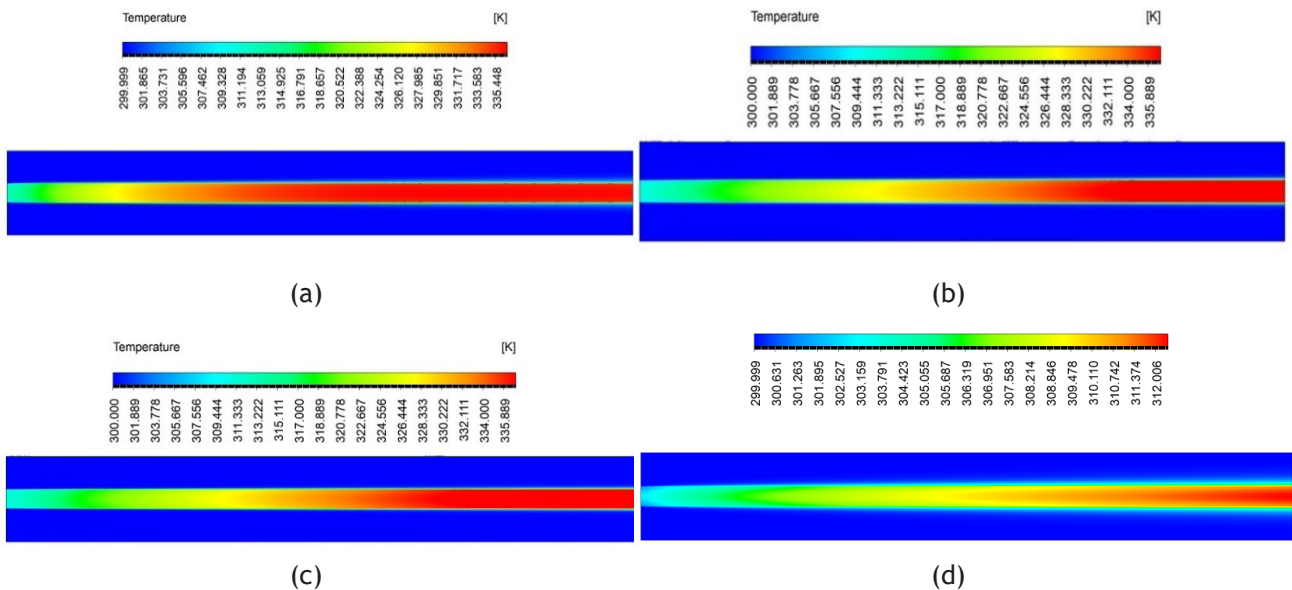


Figure 5. The temperature distribution along the annular tube with porous diameter 3mm and porosity 0,4 with materials (a)smooth (b)ceramic (c) plastic (d) steel

The temperature distribution of plastic, ceramic, and steel balls with diameters of 3, 5, and 6 (mm). The contours of the temperature distribution show that its increase as the diameter of the particles decreases. This is because a decrease in particle diameter increases the number of particles in contact with the inner cylinder and therefore transmits the heat more effectively.

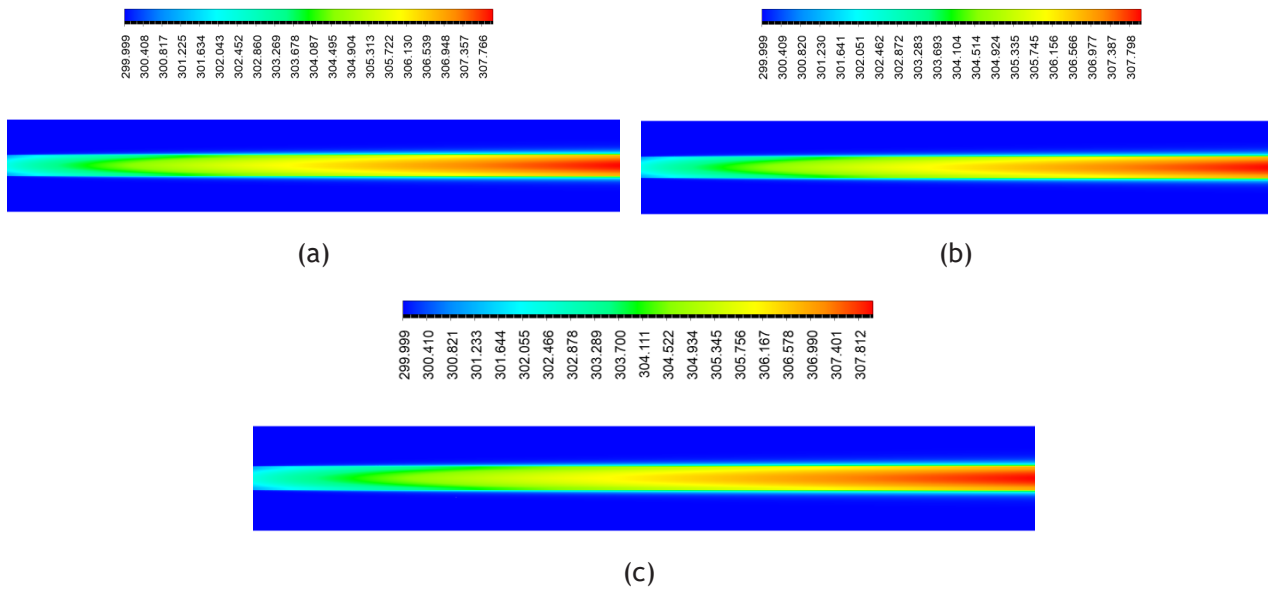
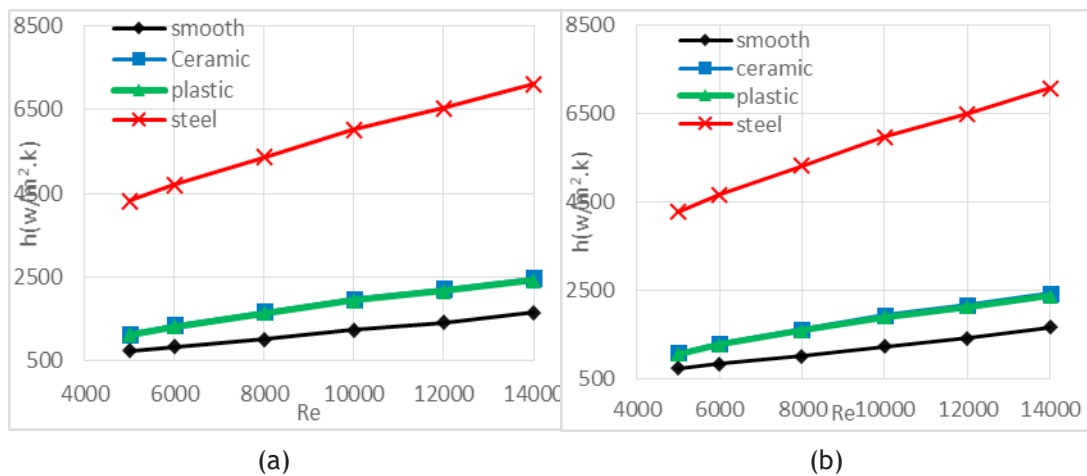


Figure 6. The temperature contours of the steel balls with (a) 3mm,(b) 5mm,(c) 6mm diameters

**Effect of diameter**

In a study, three different types of balls made of plastic, ceramic, and steel, each with diameters of 3mm, 5mm, and 6mm, were used to examine their effect on the hydraulic and thermal performance of a concentric annular tube filled with a porous medium. The variable aspects were the different materials and diameters, while the porosity was constant at a value of 0,4 for the first case. Figure 7 displays the change in heat transfer coefficient (h) with Reynold number Re for the annular tube filled with plastic, ceramic, and steel balls of different thermal conductivity (16 W/m.K for steel, 0,23 W/m.K for ceramic, and 0,16 for plastic (PVC)) as well as different diameters (3, 5, and 6) mm for each. The study showed that the heat transfer coefficient increases with increasing velocity at a constant heat flux of 33113 w/m<sup>2</sup>,<sup>(28)</sup> with and without porous medium. From the figures, it is evident that the porous medium with steel balls produces a higher heat transfer coefficient than plastic and ceramic. Moreover, for different diameters, plastic balls were found to have the lowest values of heat transfer coefficient due to the lower thermal conductivity of plastic (PVC) and ceramic as compared to steel.<sup>(29)</sup>



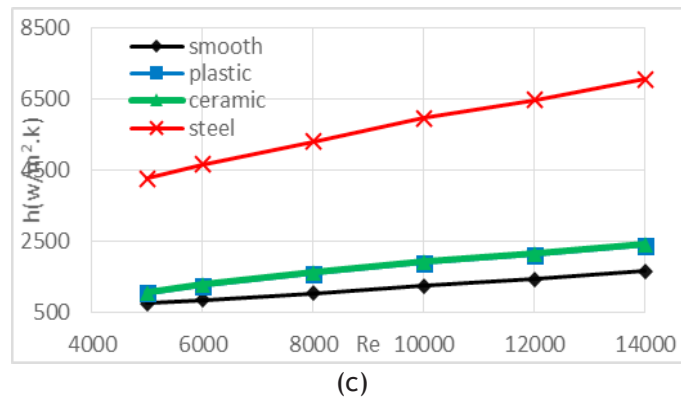


Figure 7. The effect of change in the material on the heat transfer coefficient with spheres diameters of (a)3mm,(b)5mm, and (c)6 mm and porosity of 0,4

The result of change the diameter of porous balls show that the decrease in balls diameter led to increase in heat transfer coefficient as shown in the figure 8 because the smallest size make up a higher heat exchanger area. (29,30)

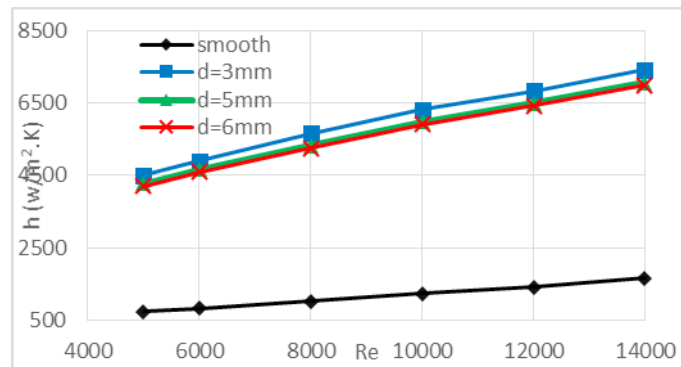


Figure 8. The effect of diameter changes for the steel ball on heat transfer coefficient

Water pressure distribution in the annular tube in the (y,z) plane is shown in figure 9. Pressure is much higher at the entrance than at the exit, where it drops to zero Pascals. Adding sphere balls increases pressure drop inversely proportionate to sphere diameter. As demonstrated in figure 9, a 3 mm sphere has a higher pressure than a 5mm or 6mm one. The lower ball diameter means less space between the spheres, requiring more pumping power.

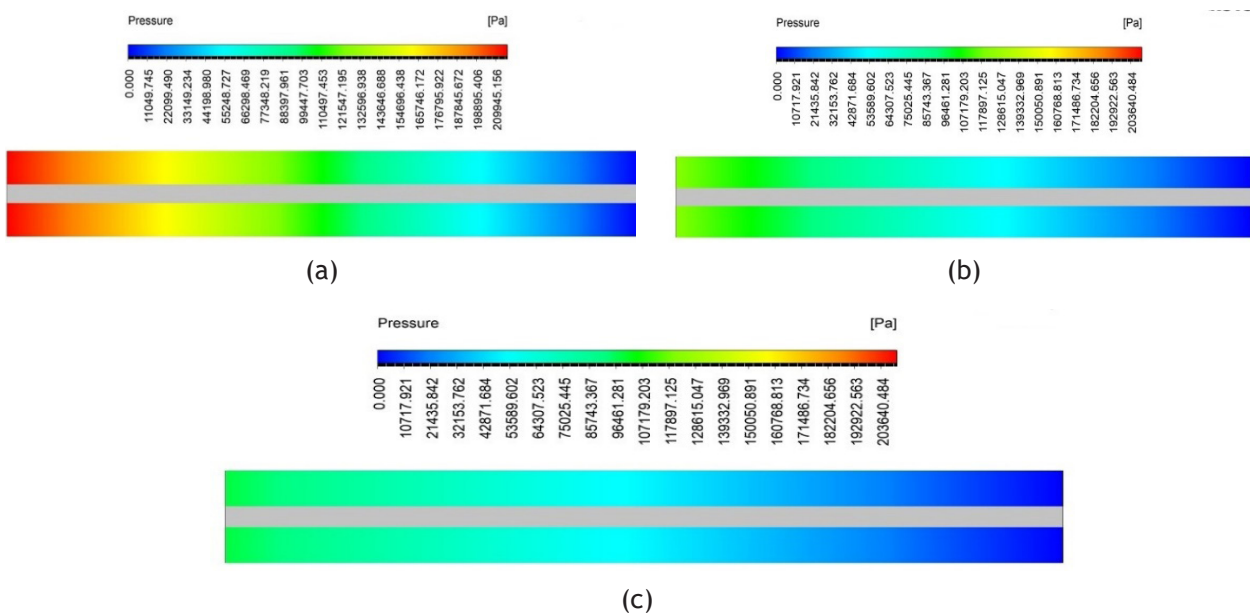


Figure 9. The pressure drop of spheres with diameters (a) 3mm, (b)5mm and (c) 6mm

**Effect of porosity**

This study examined the heat transfer coefficient in an annular tube filled with a porous media at three porosities (0,4, 0,6, and 0,8). While porosity changed, the porous medium's diameter remained 6mm. Reynolds number effects on heat transfer coefficient in annular tube filled with steel balls are shown in figure 10. At 33113 w/m<sup>2</sup>, heat flux was constant. Figure 10 illustrates that Reynolds number increases heat transfer coefficient in porous and non-porous materials. Heat transfer coefficients were lower without the porous media in the annular tube and higher with it. Low steel spherical porosity increased heat transfer coefficient. Due to steel balls' strong conductivity inside the annular tube, 0,4 porosity had the maximum heat transfer coefficient.

As seen in figure 11, annular tube pressure drop increases with Reynolds number (Re). Pressure drop is larger with low porosity (0,4) and decreases with higher porosity. This indicates that 0,6 and 0,8 porosity levels have lower pressure drops than 0,4.

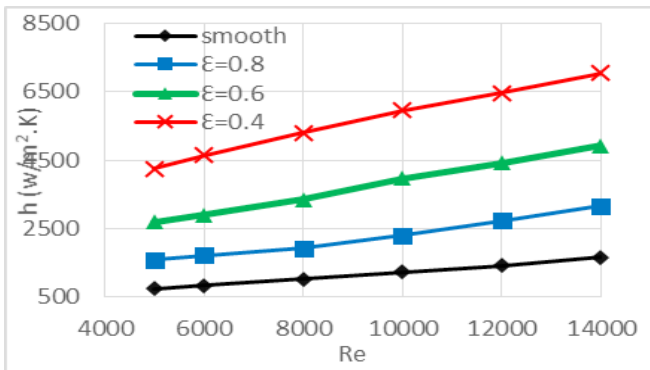


Figure 10. The effect of porosity on heat transfer coefficient

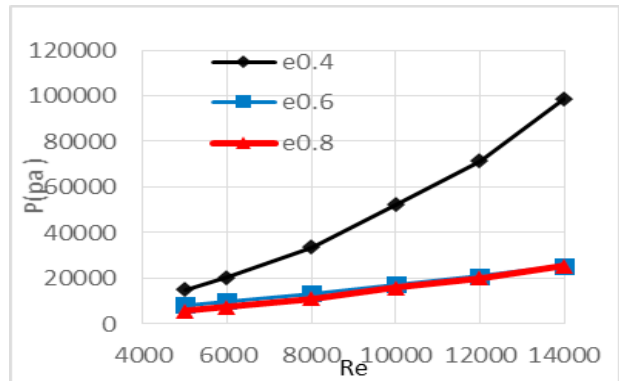
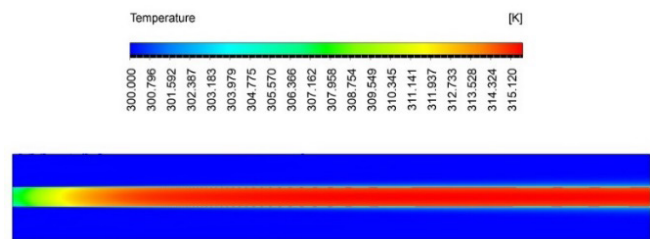
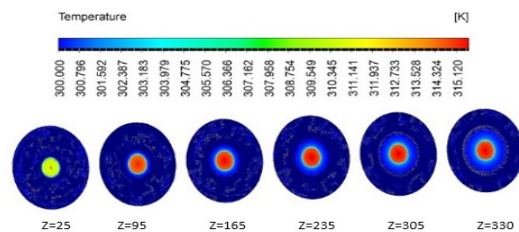


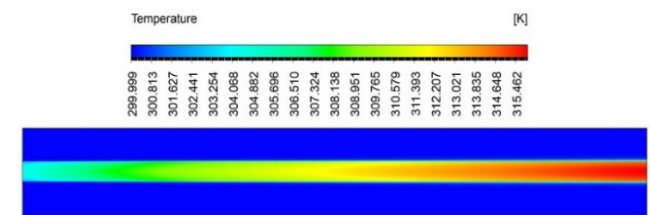
Figure 11. effect porosity on pressure drop



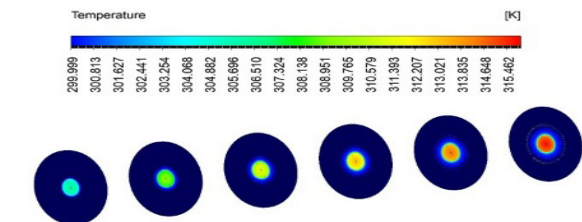
(a)



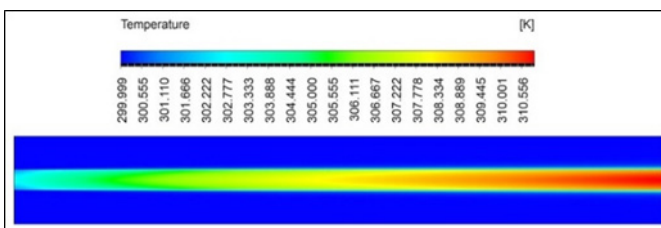
smooth



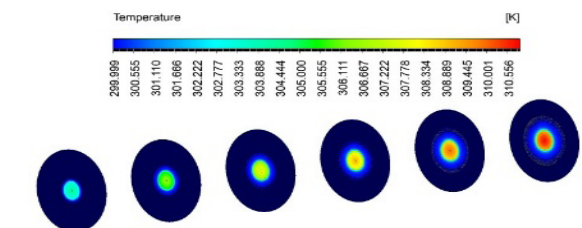
(b)



ε= (0,8)



(c)



ε= (0,6)

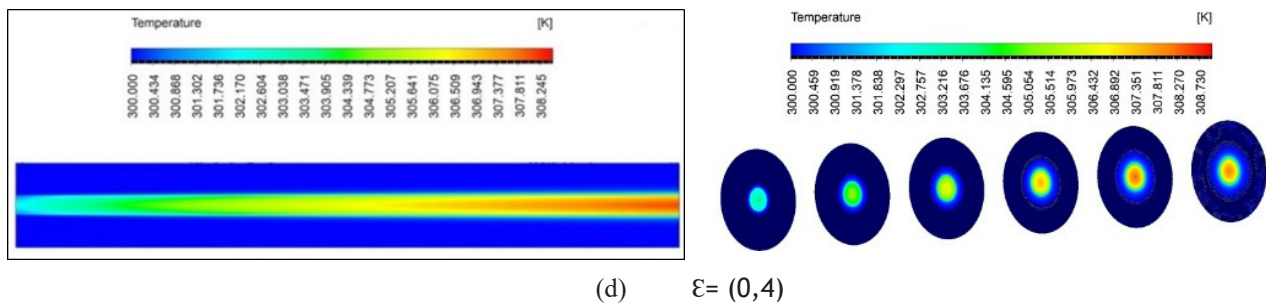


Figure 12. The effect of porosity value on temperature distribution (a) clear tube (b)  $\epsilon=0,8$  (c)  $\epsilon=0,6$  (d)  $\epsilon=0,4$

The temperature distribution through the annular tube is effected by porosity value, as shown in figure 12. The insert of sphere balls increases the temperature distribution, which is reversely proportional to porosity value. Small porosity values 0,4 have a higher temperature distribution than 0,6 and 0,8.

## CONCLUSIONS

A study examines the impact of porous materials on forced convective heat transfer in water and inner tubes in an annulus, analyzing Reynolds numbers from 5000 to 14000 and heat flux of 33113 W/m<sup>2</sup> using PVC, ceramic, and steel packed beds. The main conclusion can be listed as follows:

- 1- The fluid flow pressure drops considerably when the diameter of solid particles increases from 3 mm to 6 mm.
- 2- Fluid temperature rises more quickly in the direction of flow as velocity rises, and temperature gradients rise when isotherm lines approach cylinder surfaces, according to this analysis.
- 3- The fluid thermal boundary layer surrounding the cylinders is thick in the cases with porosity (0,4). Porous material improves heat transfer from the cylinder surface to water.
- 4- The thermal conductivity of steel balls is higher than that of PVC and ceramic. Therefore, steel balls provide better heat transmission than the other materials.
- 5- Increasing the water velocity from 0,102 m/s to 0,285 m/s also increases heat transmission.
- 6- The heat transfer coefficient of steel balls Increased by about 79 %, 69 %, and 49 %, with 0,4, 0,6, and 0,8 respectively.

## REFERENCES

1. R. Bradean, P. J. Heggs, D. B. Ingham, and I. Pop, in *Transp. Phenom. Porous Media* (Elsevier, 1998), pp. 411-438.
2. R. Lochan, R. Lochan, H. M. Sharma, and D. Agarwal, *Int. J. Innov. Res. Eng. Manag.* 3, 468 (2016).
3. H. K. Dawood, H. A. Mohammed, N. A. Che Sidik, K. M. Munisamy, and M. A. Wahid, *Int. Commun. Heat Mass Transf.* 62, 45 (2015).
4. P. H. Jadhav, N. Gnanasekaran, and M. Mobedi, *Energy* 263, 125691 (2023).
5. S. Wang, C. Xu, W. Liu, and Z. Liu, *Energies* 12, 414 (2019).
6. K. S. Bibin and J. S. Jayakumar, *Int. J. Heat Mass Transf.* 148, 119079 (2020).
7. J. Yang, L. Zhou, Y. Hu, S. Li, and Q. Wang, *Heat Transf. Eng.* 39, 1582 (2018).
8. S. Li, L. Zhou, J. Yang, and Q. Wang, *Energies* 11, 937 (2018).
9. S. Aksornkitti, P. Rattanadecho, and T. Wessapan, *Case Stud. Therm. Eng.* 28, 101417 (2021).
10. W. Maid, K. H. Hilal, and N. S. Lafta, *IOP Conf. Ser. Mater. Sci. Eng.* 745, 012081 (2020).
11. Badruddin, A. A. A. Al-Rashed, N. J. Salman Ahmed, and S. Kamangar, *Int. J. Heat Mass Transf.* 55, 2184 (2012).
12. W. Zhang, X. Bai, M. Bao, and A. Nakayama, *Appl. Therm. Eng.* 145, 735 (2018).

13. M. T. Pamuk and M. Özdemir, *Exp. Therm. Fluid Sci.* 42, 79 (2012).
14. H. Xu, C. Zhao, and K. Vafai, *Heat Mass Transf.* 53, 2663 (2017).
15. H. N. Abdulkareem and K. H. Hilal, *Wasit J. Eng. Sci.* 8, 31 (2020).
16. Mohammad Saleh, S. Rasheed, and R. Smasem, *Kufa J. Eng.* 9, 57 (2018).
17. T. H. Farhan, O. T. Fadhil, and H. E. Ahmed, *Anbar J. Eng. Sci.* 12, 100 (2021).
18. O. H. Hassan, G. I. Sultan, M. N. Sabry, and A. A. Hegazi, *Case Stud. Therm. Eng.* 32, 101849 (2022).
19. S. A. Rasheed and J. M. Abood, (2017).
20. M. F. Yousif, S. N. Shehab, and H. M. Jaffal, (n.d.).
21. D. A. Nield and A. Bejan, *Convection in Porous Media* (Springer International Publishing, Cham, 2017).
22. Bejan and A. D. Kraus, *Heat Transfer Handbook* (J. Wiley, New York, 2003).
23. M. Kaviany, *Principles of Heat Transfer in Porous Media* (Springer US, New York, NY, 1991).
24. M. F. Yousif, S. N. Shehab, and H. M. Jaffal, *J. Adv. Res. Fluid Mech. Therm. Sci.* 75, 94 (2020).
25. L. Davidson, (n.d.).
26. Y. Nakasone, S. Yoshimoto, and T. A. Stolarski, *Engineering Analysis with ANSYS Software* (Butterworth-Heinemann, Amsterdam ; Boston, 2006).
27. S. Ali and S. Rasheed, *Int. J. Nonlinear Anal. Appl.* 14, (2023).
28. R. Lochan and H. M. Sharma, *Int. J. Adv. Eng. Res. Sci.* 3, 88 (2016).
29. Ali, I. Koc, and E. F. Abbas, 9, (2020).
30. E. Khudhair and D. Khudhur, *J. Eng. Sustain. Dev.* 27, 565 (2023).

#### **FINANCING**

The authors did not receive financing for the development of this research.

#### **CONFLICT OF INTEREST**

The authors declare that there is no conflict of interest.

#### **AUTHORSHIP CONTRIBUTION**

*Conceptualization:* Noor Sabah Falieh, Saad Najeeb Shehab.

*Data curation:* Noor Sabah Falieh, Saad Najeeb Shehab.

*Formal analysis:* Noor Sabah Falieh, Saad Najeeb Shehab.

*Research:* Noor Sabah Falieh, Saad Najeeb Shehab.

*Methodology:* Noor Sabah Falieh, Saad Najeeb Shehab.

*Drafting - original draft:* Noor Sabah Falieh, Saad Najeeb Shehab.

*Writing - proofreading and editing:* Noor Sabah Falieh, Saad Najeeb Shehab.